THE ASTROPHYSICAL JOURNAL, 524:1122–1130, 1999 October 20

RATE COEFFICIENTS FOR RO-VIBRATIONAL TRANSITIONS IN H_2 DUE TO COLLISIONS WITH He

N. BALAKRISHNAN, M. VIEIRA,[1] J. F. BABB, AND A. DALGARNO
Institute for Theoretical Atomic and Molecular Physics, Harvard-Smithsonian Center for Astrophysics, 60 Garden Street, Cambridge, MA 02138
R. C. FORREY
Penn State University, Berks-Lehigh Valley College, Reading, PA 19610-6009
AND
S. LEPP
Department of Physics, 4505 South Maryland Parkway, University of Nevada, Las Vegas, NV 89154
Received 1999 February 16; accepted 1999 June 8

ABSTRACT

We present quantum mechanical and quasi-classical trajectory calculations of cross sections for ro-vibrational transitions in ortho- and para-H_2 induced by collisions with He atoms. Cross sections were obtained for kinetic energies between 10^{-4} and 3 eV, and the corresponding rate coefficients were calculated for the temperature range 100 K $\leq T \leq$ 4000 K. Comparisons are made with previous calculations.

Subject headings: molecular data — molecular processes

1. INTRODUCTION

Ro-vibrationally excited H_2 molecules have been observed in many astrophysical objects (for recent studies, see Weintraub et al. 1998; van Dishoeck et al. 1998; Shupe et al. 1998; Bujarrabal et al. 1998; Stanke, McCaughrean, & Zinnecker 1998). The ro-vibrational levels of the molecule may be populated by ultraviolet pumping, by X-ray pumping, by the formation mechanism, and by collisional excitation in shock-heated gas (Dalgarno 1995). The excited level populations are then modified by collisions followed by quadrupole emissions. The main colliding partners apart from H_2 are H and He. Although He is only 1/10 as abundant as H, collisions with He may have a significant influence in many astronomical environments depending on the density, temperature, and the initial rotational and vibrational excitation of the molecule. Collisions with He and H_2 are particularly important when most of the hydrogen is in molecular form, as in dense molecular clouds. To interpret observations of the radiation emitted by the gas, the collision cross sections and corresponding rate coefficients characterizing the collisions must be known. Emissions from excited ro-vibrational levels of the molecule provide important clues regarding the physical state of the gas, dissociation, excitation, and formation properties of H_2. Here we investigate the collisional relaxation of vibrationally excited H_2 by He.

Ro-vibrational transitions in H_2 induced by collisions with He atoms have been the subject of a large number of theoretical calculations in the past (Alexander 1976, 1977; Alexander & McGuire 1976; Dove, Raynor, & Teitelbaum 1980; Eastes & Secrest 1972; Krauss & Mies 1965; McGuire & Kouri 1974; Raczkowski, Lester, & Miller 1978) and continue to attract experimental (Audibert et al. 1976; Michaut et al. 1998) and theoretical attention (Flower, Roueff, & Zeippen 1998; Dubernet & Tuckey 1999; Balakrishnan, Forrey, & Dalgarno 1999). Recent theoretical calculations are motivated by the availability of more accurate representations of the interaction potentials and the possibility of performing quantum mechanical calculations with few approximations. The potential energy surface determined by Muchnick & Russek (1994) was used by Flower et al. (1998) and by Balakrishnan et al. (1999) in recent quantum mechanical calculations of ro-vibrational transition rate coefficients for temperatures ranging from 100 to 5000 K. Flower et al. presented their results for vibrational levels $v = 0$,1, and 2 of ortho- and para-H_2. Balakrishnan et al. (1999) reported similar results for $v = 0$ and 1. Although both authors have adopted similar close coupling approaches for the scattering calculations, Flower et al. used a harmonic oscillator approximation for H_2 vibrational wave functions in evaluating the matrix elements of the potential, while the calculations of Balakrishnan et al. made use of the H_2 potential of Schwenke (1988) and the corresponding numerically determined wave functions. The results of the two calculations agreed well for pure rotational transitions, but some discrepancies were seen for ro-vibrational transitions. We believe that this may be due to the different choice of vibrational wave functions. The sensitivity of the rate coefficients to the choice of the H_2 wave function was noted previously, and differences could be significant for excited vibrational levels. We find this to be the case for transitions involving $v \geq 2$. Thus, in this article, we report rate coefficients for transitions from $v = 2$ to 6 initial states of H_2 induced by collisions with He atoms using numerically exact quantum mechanical calculations. We also report results of quasi-classical trajectory (QCT) calculations and examine the suitability of classical mechanical calculations in predicting ro-vibrational transitions in H_2.

2. RESULTS

The quantum mechanical calculations were performed using the nonreactive scattering program MOLSCAT developed by Hutson & Green (1994) with the He-H_2 interaction potential of Muchnick & Russek (1994) and the H_2 potential of Schwenke (1988). We refer to our earlier paper (Balakrishnan et al. 1999) for details of the numerical implementation. Different basis sets were used in the calculations for transitions from different initial vibrational levels. We use the notation $[v_1{-}v_2](j_1{-}j_2)$ to represent the basis set,

[1] Present address: Department of Physics and Astronomy, University of Rochester.

where the quantities within the square brackets give the range of vibrational levels and those in parentheses give the range of rotational levels coupled in each of the vibrational levels. For transitions from $v = 2,3$, and 4 we used, respectively, the basis sets [0–3](0–11) and [4](0–3); [0–3](0–11) and [4](0–9); and [3–5](0–11) and [1, 6](0–11). For $v = 5$ and 6 of para-H_2 we used, respectively, [4–6](0–14) and [3, 7](0–8); and [5–7](0–14) and [4, 8](0–8). During the calculations, we found that the $\Delta v = \pm 2$ transitions are weak, with cross sections that are typically orders of magnitude smaller than for the $\Delta v = \pm 1$ transitions. Thus, for $v = 5$ and 6 of ortho-H_2, we have only included the $\Delta v = \pm 1$ vibrational levels with $j = 0$–13 in the basis set to reduce the computational effort. The basis sets were chosen as a compromise between numerical efficiency and accuracy and could introduce some truncation errors for transitions to levels which lie at the outer edge of the basis set. Our convergence tests show that truncation errors are small. Ro-vibrational transition cross sections $\sigma_{vj,v'j'}$, where the pairs of numbers vj and $v'j'$, respectively, denote the initial and final ro-vibrational quantum numbers, were computed for kinetic energies ranging from 10^{-4} to 3 eV. Sufficient total angular momentum partial waves were included in the calculations to secure convergence of the cross sections.

The quasi-classical calculations were carried out using the standard classical trajectory method as described by Lepp, Buch, & Dalgarno (1995) in which the procedure of Blais & Truhlar (1976) was adopted for the final state analysis. Because ro-vibrational transitions are rare at low velocities, useful results could be obtained only for collisions at energies above 0.1 eV. The results are averages over 10,000 trajectories. The quantum mechanical calculations were performed using MOLSCAT (Hutson & Green 1994), suitably adapted for the present system with the potential represented by a Legendre polynomial expansion in which we retained nonvanishing terms of orders 0–10 inclusive.

Calculation of ro-vibrational transition rate coefficients over a wide range of temperatures requires the determination of scattering cross sections at the energies spanned by the Boltzmann distribution at each temperature. This is a computationally demanding problem especially when quantum mechanical calculations are required. For many systems, QCT calculations offer a good compromise between accuracy and computational effort. However, the validity of classical mechanics is in question especially for lighter systems and at lower temperatures, where quantum mechanical effects such as tunneling are important. Because of the small masses of the atoms involved, the present

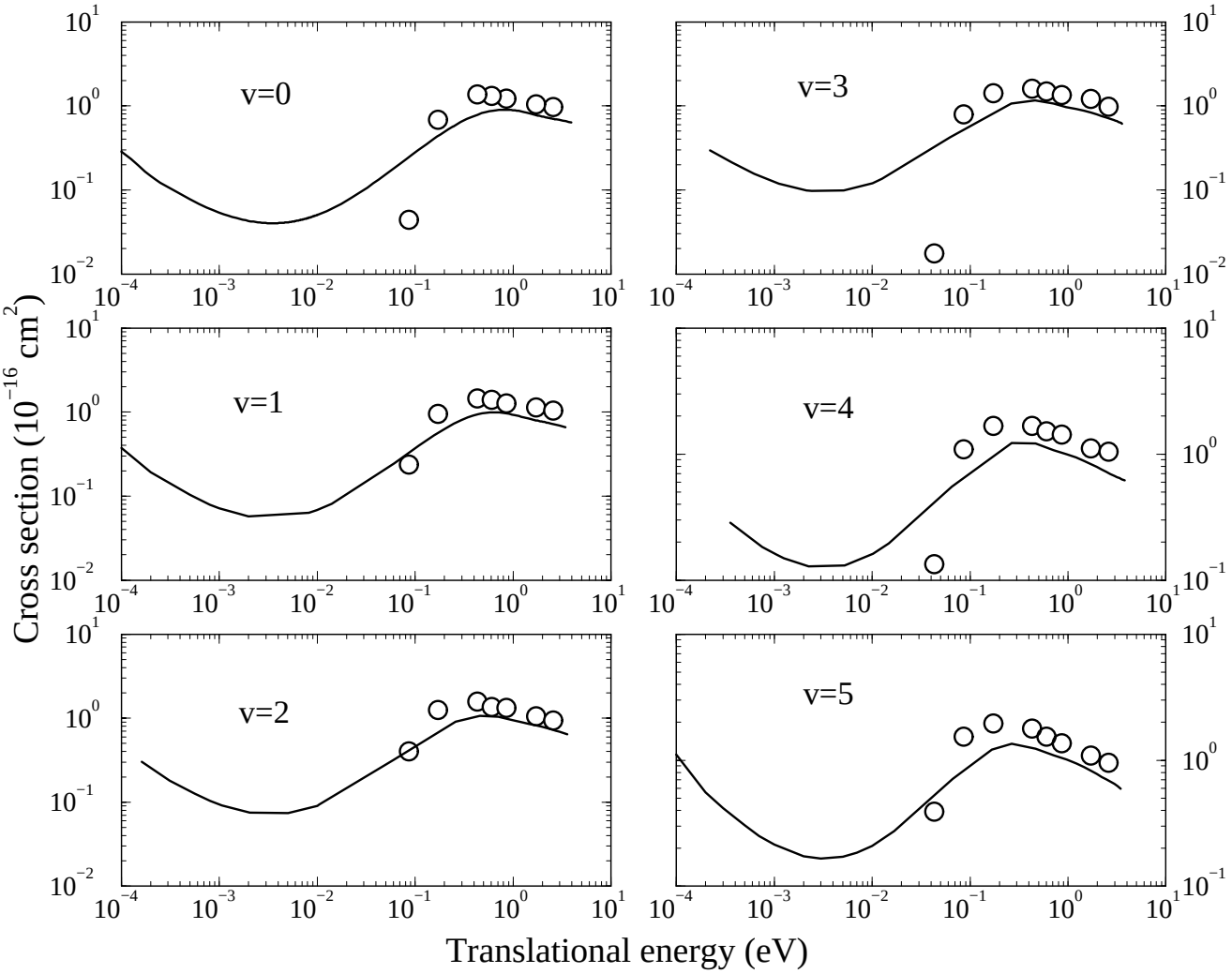

FIG. 1.—Comparison of quantum mechanical (*solid line*) and quasi-classical cross sections (*open circles*) for the $\Delta j = -2$ rotational transition from the $j = 2$ initial rotational level of H_2 in vibrational levels $v = 0$–5. The error bar for the classical mechanical results is largest for the lowest energy where it is of the size of the symbol.

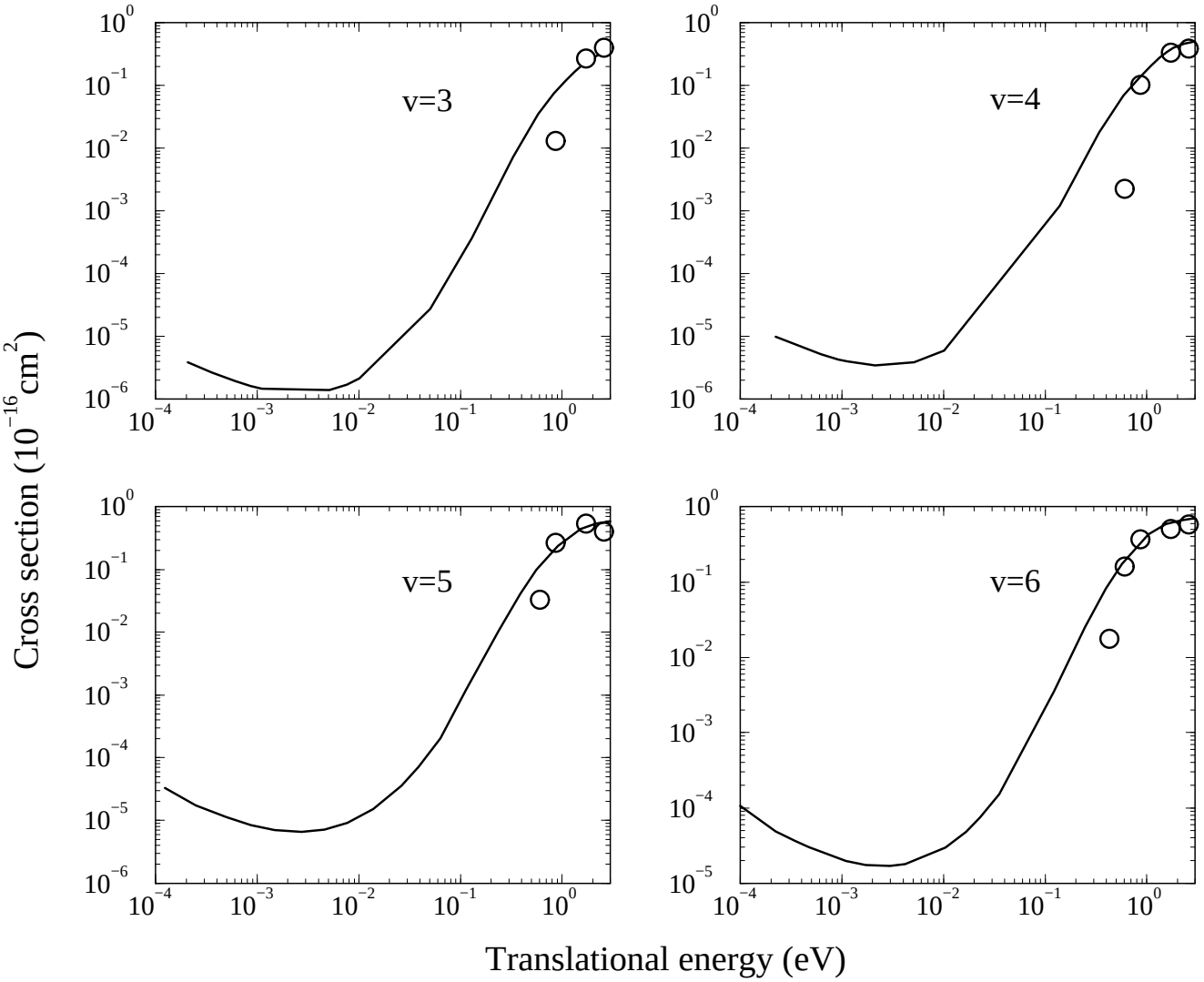

FIG. 2.—Comparison of quantum mechanical (*solid line*) and quasi-classical cross sections (*open circles*) for the $\Delta j = +2$, $\Delta v = -1$ ro-vibrational transition from the $j = 5$ initial rotational level of H_2 in vibrational levels $v = 3$–6. The error bar for the classical mechanical results is largest for the lowest energy where it is of the size of the symbol.

system offers an excellent opportunity to test the reliability of QCT calculations in predicting ro-vibrational transitions. Although such attempts have been made in the past (Dove et al. 1980) the classical mechanical and quantum mechanical calculations were done in different energy regimes, and a one-to-one comparison was not possible.

We carried out quantum mechanical and QCT calculations of ro-vibrational transition cross sections for the present system over a wide range of energies. In Figure 1 we compare the results for pure rotational de-excitation transitions ($\Delta j = j' - j = -2$) with $j = 2$ in $v = 0$–5. There are striking similarities and differences between the quantum mechanical and QCT results. They agree quite well at higher energies and have a similar energy dependence with both calculations predicting the same maximum for the cross sections before they fall off. In contrast, the agreement becomes less satisfactory at lower energies with the QCT cross sections rapidly decreasing to zero as the energy is decreased. The quantum mechanical results pass through minima and subsequently increase with further decrease of the kinetic energy. This is a purely quantum mechanical effect that has important consequences for the low temperature rate coefficients (Balakrishnan et al. 1998). The quantum mechanical cross sections eventually conform to an inverse velocity dependence as the relative translational energy is decreased to zero and the corresponding rate coefficients are finite in the limit of zero temperature, in accordance with Wigner's threshold law. The results illustrate that QCT calculations may be used reliably to calculate rotational transitions for energies higher than 0.5 eV, but at lower energies, quantum mechanical calculation must be employed. The energy regime for the validity of QCT results is more restricted for ro-vibrational transitions, as illustrated in Figure 2 in which we show cross sections for ro-vibrational transitions $v, j \rightarrow v - 1, j + 2$ with $j = 5$ in $v = 3$–5. The results indicate that the QCT method is inadequate to calculate ro-vibrational transition cross sections at impact energies below 1 eV. The QCT results exhibit a sharp fall below a threshold near an energy of 1 eV, whereas the quantum mechanical results vary smoothly. Similar results hold for other transitions. The higher collision energies required for the validity of the QCT method for ro-vibrational transitions compared with pure rotational transitions is due in part to the much smaller cross sections

TABLE 1

A Comparison of Rate Coefficients (in Units of cm^3 s^{-1}) for Collisionally Induced Ro-vibrational Transitions in Para-H_2 Computed in This Paper and Those of Flower et al. (1998) at $T = 1000$ K

vj, $v'j'$	This Work	Flower et al.
20, 10	1.24(−15)	1.1(−15)
20, 12	2.03(−15)	2.6(−15)
20, 14	3.65(−15)	3.7(−15)
20, 16	3.28(−15)	1.3(−15)
20, 18	7.75(−16)	1.6(−16)
22, 10	3.64(−16)	3.4(−16)
22, 12	2.87(−15)	2.8(−15)
22, 14	8.05(−15)	7.2(−15)
22, 16	5.16(−15)	4.2(−15)
22, 18	2.14(−15)	6.3(−16)
22, 20	2.45(−11)	1.8(−11)
21, 11	1.82(−15)	1.8(−15)
21, 13	4.38(−15)	4.6(−15)
21, 15	3.95(−15)	3.4(−15)
21, 17	2.52(−15)	8.0(−16)
23, 11	9.48(−16)	8.6(−16)
23, 13	4.42(−15)	3.7(−15)
23, 15	1.41(−14)	1.2(−14)
23, 17	1.19(−14)	7.7(−15)
23, 21	2.55(−11)	1.8(−11)

for ro-vibrational transitions, making the results more sensitive to the details of the dynamics.

Rate coefficients $k_{vj,v'j'}(T)$ were calculated for the temperature range $T = 100$–4000 K by averaging the cross sections over a Boltzmann distribution of relative velocities. Flower et al. (1998) have reported rate coefficients for ro-vibrational transitions from $v = 0$ to 2 for $T = 1000$, 2000, and 4500 K. A comparison of some of the de-excitation rate coefficients from the $v = 2$ level calculated in this paper and those reported by Flower et al. is given in Table 1 for $T = 1000$ K. The agreement is good for ro-vibrational transitions involving $|\Delta j| = 0$,2, and 4, but larger differences, by factors between 2 and 4, are seen for transitions involving larger values of $|\Delta j|$. Our rate coefficients are generally greater than those of Flower et al. (1998) for transitions where the discrepancy is large. Our rate coefficient calculations extend those of Flower et al. (1998) to include the $v = 4$, 5, and 6 vibrational levels. The preferential formation of H_2 in these vibrational levels has been discussed by Dalgarno (1995).

In Tables 2 and 3, we present our comprehensive results for ro-vibrational de-excitation transitions from different rotational levels in para- and ortho-H_2 from the $v = 2$ level as functions of temperature. The corresponding excitation rate coefficients may be obtained from detailed balance:

$$k_{v'j',v,j}(T) = \frac{(2j+1)}{(2j'+1)} \exp\left[\frac{(\epsilon_{v'j'} - \epsilon_{vj})}{k_B T}\right] k_{vj,v'j'}(T) , \quad (1)$$

where k_B is the Boltzmann constant and ϵ_{vj} is the ro-vibrational energy of the molecule in the v, j level. Similar results for $v = 3$–6 are presented in Tables 4–11. Tables 2–11 reveal some interesting aspects of energy transfer. It can be seen that for temperatures less than 1000 K, rate

TABLE 2

Rate Coefficients (in Units of cm^3 s^{-1}) for Collisionally Induced Ro-vibrational Transitions in Para-H_2 at Different Values of the Translational Temperature T

	T (K)							
vj, $v'j'$	100	200	300	500	1000	2000	3000	4000
20, 10	2.81(−19)	2.27(−18)	9.84(−18)	7.51(−17)	1.24(−15)	1.67(−14)	6.93(−14)	1.80(−13)
20, 12	9.72(−19)	6.91(−18)	2.80(−17)	1.76(−16)	2.03(−15)	2.44(−14)	1.05(−13)	2.80(−13)
20, 14	1.05(−19)	1.36(−18)	9.47(−18)	1.29(−16)	3.65(−15)	5.64(−14)	2.11(−13)	4.88(−13)
20, 16	1.39(−18)	8.83(−18)	3.23(−17)	1.94(−16)	3.28(−15)	6.83(−14)	3.10(−13)	7.69(−13)
20, 18	1.20(−19)	9.40(−19)	2.56(−18)	1.96(−17)	7.75(−16)	2.92(−14)	2.03(−13)	6.54(−13)
22, 10	6.41(−20)	2.14(−19)	8.50(−19)	1.27(−17)	3.64(−16)	6.39(−15)	2.67(−14)	6.62(−14)
22, 12	6.45(−19)	2.72(−18)	1.09(−17)	1.26(−16)	2.87(−15)	4.25(−14)	1.70(−13)	4.19(−13)
22, 14	2.89(−18)	1.80(−17)	7.27(−17)	5.46(−16)	8.05(−15)	8.79(−14)	3.06(−13)	6.87(−13)
22, 16	3.88(−18)	2.36(−17)	8.03(−17)	3.99(−16)	5.16(−15)	8.97(−14)	3.82(−13)	9.27(−13)
22, 18	4.49(−17)	8.25(−17)	1.17(−16)	2.38(−16)	2.14(−15)	4.58(−14)	2.71(−13)	8.12(−13)
22, 20	1.68(−12)	3.71(−12)	5.98(−12)	1.10(−11)	2.45(−11)	4.69(−11)	6.24(−11)	7.36(−11)
24, 10	9.46(−21)	7.68(−20)	4.14(−19)	4.68(−18)	1.60(−16)	3.91(−15)	1.87(−14)	4.86(−14)
24, 12	1.14(−19)	9.15(−19)	4.70(−18)	4.86(−17)	1.41(−15)	2.82(−14)	1.22(−13)	2.99(−13)
24, 14	8.87(−19)	6.94(−18)	3.26(−17)	2.88(−16)	6.16(−15)	9.36(−14)	3.61(−13)	8.44(−13)
24, 16	1.02(−17)	7.03(−17)	2.81(−16)	1.90(−15)	2.53(−14)	2.52(−13)	8.10(−13)	1.72(−12)
24, 18	2.63(−16)	1.08(−15)	2.71(−15)	8.61(−15)	3.62(−14)	1.90(−13)	6.59(−13)	1.55(−12)
24, 20	9.46(−15)	3.58(−14)	8.74(−14)	2.83(−13)	1.32(−12)	4.83(−12)	8.72(−12)	1.22(−11)
24, 22	2.98(−13)	9.52(−13)	2.02(−12)	5.31(−12)	1.82(−11)	4.96(−11)	7.85(−11)	1.03(−10)
26, 10	1.11(−21)	1.15(−20)	6.67(−20)	8.71(−19)	4.39(−17)	1.69(−15)	1.03(−14)	3.09(−14)
26, 12	1.26(−20)	1.27(−19)	7.17(−19)	8.90(−18)	3.93(−16)	1.29(−14)	7.14(−14)	2.00(−13)
26, 14	1.13(−19)	1.04(−18)	5.57(−18)	6.14(−17)	2.03(−15)	4.86(−14)	2.27(−13)	5.77(−13)
26, 16	1.60(−18)	1.29(−17)	6.08(−17)	5.44(−16)	1.18(−14)	1.84(−13)	7.02(−13)	1.60(−12)
26, 18	5.89(−17)	3.70(−16)	1.37(−15)	8.29(−15)	9.59(−14)	8.22(−13)	2.35(−12)	4.50(−12)
26, 110	1.31(−14)	3.07(−14)	5.17(−14)	9.89(−14)	2.22(−13)	5.31(−13)	1.29(−12)	2.72(−12)
26, 20	6.77(−17)	3.80(−16)	1.28(−15)	6.85(−15)	6.87(−14)	5.18(−13)	1.34(−12)	2.31(−12)
26, 22	1.42(−15)	7.24(−15)	2.21(−14)	1.02(−13)	8.00(−13)	4.63(−12)	1.05(−11)	1.68(−11)
26, 24	4.64(−14)	1.86(−13)	4.60(−13)	1.55(−12)	7.81(−12)	2.96(−11)	5.41(−11)	7.68(−11)

TABLE 3

SAME AS TABLE 2, BUT FOR ORTHO-H_2

	T (K)							
vj, $v'j'$	100	200	300	500	1000	2000	3000	4000
21, 11	2.45(−19)	2.25(−18)	1.04(−17)	9.14(−17)	1.82(−15)	2.75(−14)	1.16(−13)	2.97(−13)
21, 13	1.42(−18)	1.09(−17)	4.66(−17)	3.28(−16)	4.38(−15)	4.69(−14)	1.72(−13)	4.12(−13)
21, 15	6.32(−19)	4.64(−18)	1.60(−17)	1.32(−16)	3.95(−15)	7.51(−14)	3.01(−13)	7.02(−13)
21, 17	8.43(−19)	5.24(−18)	2.23(−17)	1.58(−16)	2.52(−15)	5.66(−14)	2.93(−13)	7.85(−13)
21, 19	6.90(−19)	1.67(−18)	2.07(−18)	6.96(−18)	3.28(−16)	1.52(−14)	1.30(−13)	4.73(−13)
23, 11	6.70(−20)	1.04(−18)	5.29(−18)	4.16(−17)	9.48(−16)	1.74(−14)	7.33(−14)	1.80(−13)
23, 13	5.18(−19)	7.20(−18)	3.47(−17)	2.46(−16)	4.42(−15)	6.56(−14)	2.54(−13)	6.01(−13)
23, 15	4.76(−18)	2.24(−17)	1.05(−16)	9.22(−16)	1.41(−14)	1.49(−13)	5.02(−13)	1.09(−12)
23, 17	3.15(−17)	1.80(−16)	5.32(−16)	1.98(−15)	1.19(−14)	1.18(−13)	4.73(−13)	1.14(−12)
23, 19	1.74(−17)	2.64(−17)	2.44(−17)	7.30(−17)	1.81(−15)	3.76(−14)	2.34(−13)	7.32(−13)
23, 21	7.73(−13)	2.12(−12)	4.03(−12)	9.09(−12)	2.55(−11)	5.93(−11)	8.67(−11)	1.08(−10)
25, 11	3.36(−21)	1.25(−19)	6.81(−19)	8.38(−18)	3.34(−16)	9.44(−15)	4.83(−14)	1.30(−13)
25, 13	3.68(−20)	9.71(−19)	4.92(−18)	5.35(−17)	1.75(−15)	3.86(−14)	1.72(−13)	4.26(−13)
25, 15	7.05(−19)	8.96(−18)	4.23(−17)	3.76(−16)	8.51(−15)	1.31(−13)	4.98(−13)	1.14(−12)
25, 17	1.97(−17)	1.42(−16)	5.78(−16)	3.80(−15)	4.82(−14)	4.46(−13)	1.34(−12)	2.69(−12)
25, 19	1.74(−15)	5.74(−15)	1.27(−14)	3.38(−14)	1.04(−13)	3.28(−13)	8.92(−13)	1.93(−12)
25, 21	2.81(−15)	1.46(−14)	4.69(−14)	2.02(−13)	1.26(−12)	5.89(−12)	1.21(−11)	1.82(−11)
25, 23	7.59(−14)	3.04(−13)	8.30(−13)	2.83(−12)	1.21(−11)	3.86(−11)	6.57(−11)	8.97(−11)
27, 11	7.46(−22)	1.06(−20)	7.90(−20)	1.30(−18)	7.34(−17)	3.33(−15)	2.23(−14)	7.02(−14)
27, 13	6.52(−21)	8.65(−20)	6.02(−19)	8.89(−18)	4.15(−16)	1.49(−14)	8.65(−14)	2.48(−13)
27, 15	7.60(−20)	9.01(−19)	5.62(−18)	6.93(−17)	2.34(−15)	5.81(−14)	2.76(−13)	7.02(−13)
27, 17	1.22(−18)	1.71(−17)	8.62(−17)	7.31(−16)	1.59(−14)	2.49(−13)	9.32(−13)	2.07(−12)
27, 19	1.28(−16)	8.18(−16)	3.14(−15)	1.87(−14)	1.93(−13)	1.47(−12)	3.91(−12)	7.10(−12)
27, 111.....	1.41(−14)	2.79(−14)	4.96(−14)	1.10(−13)	2.76(−13)	6.45(−13)	1.51(−12)	3.12(−12)
27, 21	1.52(−17)	1.35(−16)	6.40(−16)	4.63(−15)	6.16(−14)	6.02(−13)	1.77(−12)	3.33(−12)
27, 23	2.32(−16)	1.87(−15)	8.06(−15)	4.96(−14)	4.84(−13)	3.35(−12)	8.23(−12)	1.39(−11)
27, 25	9.84(−15)	5.68(−14)	1.95(−13)	8.65(−13)	5.19(−12)	2.24(−11)	4.39(−11)	6.47(−11)

TABLE 4

SAME AS TABLE 2, BUT FOR THE $v = 3$ LEVEL OF PARA-H_2

	T (K)							
vj, $v'j'$	100	200	300	500	1000	2000	3000	4000
30, 20	1.07(−18)	8.34(−18)	3.53(−17)	2.47(−16)	3.49(−15)	4.21(−14)	1.66(−13)	4.08(−13)
30, 22	3.26(−18)	2.24(−17)	8.59(−17)	4.87(−16)	4.90(−15)	5.66(−14)	2.34(−13)	5.94(−13)
30, 24	3.10(−19)	5.35(−18)	2.79(−17)	3.64(−16)	9.40(−15)	1.21(−13)	4.20(−13)	9.36(−13)
30, 26	4.37(−18)	2.94(−17)	1.09(−16)	6.47(−16)	1.01(−14)	1.68(−13)	6.58(−13)	1.50(−12)
30, 28	4.98(−19)	3.76(−18)	1.17(−17)	9.42(−17)	3.05(−15)	9.39(−14)	5.37(−13)	1.50(−12)
32, 20	2.40(−19)	1.04(−18)	4.18(−18)	5.00(−17)	1.17(−15)	1.64(−14)	6.15(−14)	1.43(−13)
32, 22	2.00(−18)	1.08(−17)	4.43(−17)	4.24(−16)	7.98(−15)	1.01(−13)	3.78(−13)	8.92(−13)
32, 24	8.28(−18)	5.81(−17)	2.37(−16)	1.59(−15)	1.97(−14)	1.88(−13)	6.11(−13)	1.31(−12)
32, 26	1.71(−17)	9.45(−17)	3.00(−16)	1.41(−15)	1.59(−14)	2.19(−13)	8.18(−13)	1.83(−12)
32, 28	1.51(−16)	2.68(−16)	3.84(−16)	8.19(−16)	7.08(−15)	1.33(−13)	6.72(−13)	1.78(−12)
32, 30	2.10(−12)	4.67(−12)	7.63(−12)	1.41(−11)	3.00(−11)	5.35(−11)	6.87(−11)	7.93(−11)
34, 20	4.51(−20)	3.71(−19)	1.96(−18)	2.07(−17)	5.97(−16)	1.13(−14)	4.61(−14)	1.08(−13)
34, 22	4.81(−19)	3.94(−18)	1.98(−17)	1.91(−16)	4.66(−15)	7.41(−14)	2.79(−13)	6.32(−13)
34, 24	3.21(−18)	2.52(−17)	1.15(−16)	9.63(−16)	1.77(−14)	2.24(−13)	7.83(−13)	1.72(−12)
34, 26	3.09(−17)	2.08(−16)	8.09(−16)	5.18(−15)	6.15(−14)	5.39(−13)	1.62(−12)	3.27(−12)
34, 28	8.59(−16)	3.38(−15)	8.20(−15)	2.46(−14)	9.56(−14)	4.64(−13)	1.45(−12)	3.12(−12)
34, 30	1.69(−14)	6.25(−14)	1.49(−13)	4.67(−13)	2.02(−12)	6.64(−12)	1.11(−11)	1.48(−11)
34, 32	4.41(−13)	1.38(−12)	2.86(−12)	7.29(−12)	2.37(−11)	6.05(−11)	9.19(−11)	1.17(−10)
36, 20	5.40(−21)	6.41(−20)	3.79(−19)	4.77(−18)	1.99(−16)	5.90(−15)	2.96(−14)	7.69(−14)
36, 22	6.08(−20)	6.51(−19)	3.73(−18)	4.44(−17)	1.62(−15)	4.10(−14)	1.88(−13)	4.65(−13)
36, 24	5.01(−19)	4.60(−18)	2.43(−17)	2.55(−16)	7.12(−15)	1.35(−13)	5.40(−13)	1.23(−12)
36, 26	5.97(−18)	4.67(−17)	2.15(−16)	1.82(−15)	3.42(−14)	4.42(−13)	1.51(−12)	3.19(−12)
36, 28	1.71(−16)	1.06(−15)	3.81(−15)	2.18(−14)	2.26(−13)	1.69(−12)	4.48(−12)	8.16(−12)
36, 210	3.35(−14)	7.60(−14)	1.26(−13)	2.36(−13)	5.03(−13)	1.20(−12)	2.85(−12)	5.56(−12)
36, 30	1.65(−16)	9.11(−16)	3.02(−15)	1.54(−14)	1.38(−13)	8.91(−13)	2.05(−12)	3.27(−12)
36, 32	2.88(−15)	1.46(−14)	4.43(−14)	1.94(−13)	1.37(−12)	6.97(−12)	1.45(−11)	2.19(−11)
36, 34	7.49(−14)	3.00(−13)	7.43(−13)	2.41(−12)	1.09(−11)	3.75(−11)	6.50(−11)	8.92(−11)

TABLE 5

SAME AS TABLE 4, BUT FOR ORTHO-H_2

	T (K)							
vj, $v'j'$	100	200	300	500	1000	2000	3000	4000
31, 21	9.61(−19)	8.24(−18)	3.76(−17)	3.05(−16)	5.20(−15)	6.88(−14)	2.72(−13)	6.68(−13)
31, 23	4.95(−18)	3.52(−17)	1.45(−16)	9.36(−16)	1.06(−14)	1.01(−13)	3.56(−13)	8.23(−13)
31, 25	3.48(−18)	2.22(−17)	7.27(−17)	5.03(−16)	1.15(−14)	1.72(−13)	6.12(−13)	1.33(−12)
31, 27	3.94(−18)	1.97(−17)	7.89(−17)	5.43(−16)	8.16(−15)	1.51(−13)	6.61(−13)	1.58(−12)
31, 29	4.17(−18)	9.92(−18)	1.23(−17)	3.66(−17)	1.44(−15)	5.32(−14)	3.68(−13)	1.14(−12)
33, 21	3.64(−19)	3.26(−18)	1.63(−17)	1.45(−16)	3.04(−15)	4.50(−14)	1.68(−13)	3.82(−13)
33, 23	2.04(−18)	1.17(−17)	5.84(−17)	6.25(−16)	1.23(−14)	1.54(−13)	5.46(−13)	1.23(−12)
33, 25	1.50(−17)	9.82(−17)	3.93(−16)	2.69(−15)	3.41(−14)	3.19(−13)	9.97(−13)	2.05(−12)
33, 27	1.14(−16)	5.67(−16)	1.63(−15)	5.99(−15)	3.42(−14)	2.91(−13)	1.03(−12)	2.26(−12)
33, 29	7.14(−18)	5.74(−17)	1.18(−16)	4.21(−16)	6.07(−15)	1.10(−13)	5.85(−13)	1.61(−12)
33, 31	1.10(−12)	2.85(−12)	5.21(−12)	1.15(−11)	3.16(−11)	6.99(−11)	9.85(−11)	1.20(−10)
35, 21	6.90(−20)	6.45(−19)	3.58(−18)	4.15(−17)	1.32(−15)	2.84(−14)	1.22(−13)	2.91(−13)
35, 23	4.97(−19)	4.37(−18)	2.27(−17)	2.34(−16)	6.01(−15)	1.03(−13)	3.96(−13)	8.88(−13)
35, 25	4.36(−18)	3.42(−17)	1.58(−16)	1.34(−15)	2.45(−14)	3.11(−13)	1.06(−12)	2.27(−12)
35, 27	6.99(−17)	4.47(−16)	1.69(−15)	1.03(−14)	1.15(−13)	9.30(−13)	2.61(−12)	4.96(−12)
35, 29	6.11(−15)	1.88(−14)	3.81(−14)	9.04(−14)	2.52(−13)	7.54(−13)	1.89(−12)	3.77(−12)
35, 31	8.21(−15)	3.58(−14)	9.78(−14)	3.70(−13)	2.07(−12)	8.61(−12)	1.63(−11)	2.33(−11)
35, 33	1.81(−13)	6.43(−13)	1.48(−12)	4.31(−12)	1.65(−11)	4.83(−11)	7.85(−11)	1.04(−10)
37, 21	7.60(−21)	8.23(−20)	5.12(−19)	7.35(−18)	3.58(−16)	1.23(−14)	6.65(−14)	1.79(−13)
37, 23	5.66(−20)	5.81(−19)	3.41(−18)	4.40(−17)	1.76(−15)	4.82(−14)	2.30(−13)	5.67(−13)
37, 25	5.33(−19)	4.96(−18)	2.63(−17)	2.83(−16)	8.20(−15)	1.60(−13)	6.45(−13)	1.47(−12)
37, 27	8.72(−18)	6.89(−17)	3.12(−16)	2.54(−15)	4.66(−14)	5.88(−13)	1.95(−12)	4.00(−12)
37, 29	4.85(−16)	2.81(−15)	9.55(−15)	4.92(−14)	4.45(−13)	2.96(−12)	7.25(−12)	1.24(−11)
37, 211.....	4.72(−14)	1.02(−13)	1.64(−13)	2.95(−13)	6.10(−13)	1.41(−12)	3.24(−12)	6.21(−12)
37, 31	7.94(−17)	5.07(−16)	1.90(−15)	1.15(−14)	1.33(−13)	1.11(−12)	2.90(−12)	4.99(−12)
37, 33	1.04(−15)	5.91(−15)	1.99(−14)	9.99(−14)	8.52(−13)	5.17(−12)	1.16(−11)	1.84(−11)
37, 35	3.37(−14)	1.47(−13)	3.95(−13)	1.43(−12)	7.48(−12)	2.91(−11)	5.35(−11)	7.58(−11)

TABLE 6

SAME AS TABLE 2, BUT FOR THE $v = 4$ LEVEL OF PARA-H_2

	T (K)							
vj, $v'j'$	100	200	300	500	1000	2000	3000	4000
40, 30	3.80(−18)	2.84(−17)	1.15(−16)	7.34(−16)	8.72(−15)	9.41(−14)	3.45(−13)	7.93(−13)
40, 32	1.04(−17)	6.85(−17)	2.42(−16)	1.22(−15)	1.09(−14)	1.21(−13)	4.68(−13)	1.13(−12)
40, 34	3.10(−18)	2.65(−17)	1.27(−16)	1.24(−15)	2.35(−14)	2.44(−13)	7.93(−13)	1.73(−12)
40, 36	1.18(−17)	8.57(−17)	3.20(−16)	1.89(−15)	2.76(−14)	3.72(−13)	1.31(−12)	2.85(−12)
40, 38	2.13(−18)	1.25(−17)	4.47(−17)	3.58(−16)	9.81(−15)	2.64(−13)	1.31(−12)	3.27(−12)
42, 30	8.21(−19)	4.63(−18)	1.92(−17)	1.86(−16)	3.42(−15)	3.82(−14)	1.28(−13)	2.78(−13)
42, 32	5.78(−18)	3.93(−17)	1.68(−16)	1.35(−15)	2.06(−14)	2.21(−13)	7.65(−13)	1.70(−12)
42, 34	2.28(−17)	1.73(−16)	7.04(−16)	4.29(−15)	4.52(−14)	3.77(−13)	1.16(−12)	2.42(−12)
42, 36	6.41(−17)	3.31(−16)	9.85(−16)	4.34(−15)	4.36(−14)	4.83(−13)	1.63(−12)	3.46(−12)
42, 38	4.36(−16)	7.42(−16)	1.08(−15)	2.45(−15)	2.12(−14)	3.63(−13)	1.61(−12)	3.86(−12)
42, 40	2.72(−12)	5.95(−12)	9.66(−12)	1.75(−11)	3.54(−11)	5.96(−11)	7.43(−11)	8.42(−11)
44, 30	2.00(−19)	1.68(−18)	8.65(−18)	8.58(−17)	2.05(−15)	3.04(−14)	1.07(−13)	2.30(−13)
44, 32	2.09(−18)	1.45(−17)	7.15(−17)	6.85(−16)	1.41(−14)	1.80(−13)	6.08(−13)	1.29(−12)
44, 34	1.24(−17)	7.53(−17)	3.37(−16)	2.86(−15)	4.60(−14)	4.88(−13)	1.57(−12)	3.29(−12)
44, 36	9.22(−17)	5.58(−16)	2.09(−15)	1.29(−14)	1.36(−13)	1.05(−12)	2.98(−12)	5.78(−12)
44, 38	2.44(−15)	9.32(−15)	2.19(−14)	6.21(−14)	2.25(−13)	1.07(−12)	3.12(−12)	6.30(−12)
44, 40	2.93(−14)	1.07(−13)	2.52(−13)	7.51(−13)	2.96(−12)	8.63(−12)	1.35(−11)	1.73(−11)
44, 42	6.42(−13)	1.99(−12)	4.07(−12)	1.00(−11)	3.03(−11)	7.21(−11)	1.05(−10)	1.30(−10)
46, 30	3.23(−20)	3.46(−19)	2.05(−18)	2.42(−17)	8.33(−16)	1.90(−14)	8.05(−14)	1.86(−13)
46, 32	3.15(−19)	3.23(−18)	1.85(−17)	2.04(−16)	6.14(−15)	1.20(−13)	4.73(−13)	1.05(−12)
46, 34	2.08(−18)	1.97(−17)	1.04(−16)	9.95(−16)	2.30(−14)	3.49(−13)	1.22(−12)	2.54(−12)
46, 36	1.79(−17)	1.13(−16)	4.95(−16)	4.86(−15)	9.20(−14)	1.02(−12)	3.14(−12)	6.18(−12)
46, 38	4.36(−16)	2.68(−15)	9.49(−15)	5.13(−14)	4.81(−13)	3.24(−12)	8.10(−12)	1.41(−11)
46, 310.....	7.36(−14)	1.59(−13)	2.53(−13)	4.28(−13)	6.92(−13)	1.17(−12)	2.98(−12)	6.32(−12)
46, 40	3.83(−16)	2.10(−15)	6.85(−15)	3.26(−14)	2.54(−13)	1.37(−12)	2.81(−12)	4.16(−12)
46, 42	5.72(−15)	2.88(−14)	8.65(−14)	3.58(−13)	2.22(−12)	9.79(−12)	1.87(−11)	2.67(−11)
46, 44	1.19(−13)	4.67(−13)	1.15(−12)	3.59(−12)	1.49(−11)	4.63(−11)	7.61(−11)	1.01(−10)

TABLE 7

SAME AS TABLE 6, BUT FOR ORTHO-H_2

	T (K)							
vj, $v'j'$	100	200	300	500	1000	2000	3000	4000
41, 31	3.30(−18)	2.80(−17)	1.27(−16)	9.43(−16)	1.35(−14)	1.54(−13)	5.66(−13)	1.30(−12)
41, 33	1.40(−17)	1.03(−16)	4.14(−16)	2.45(−15)	2.37(−14)	2.04(−13)	6.77(−13)	1.49(−12)
41, 35	1.43(−17)	8.40(−17)	2.80(−16)	1.69(−15)	2.86(−14)	3.47(−13)	1.13(−12)	2.36(−12)
41, 37	1.52(−17)	6.71(−17)	2.50(−16)	1.66(−15)	2.33(−14)	3.56(−13)	1.37(−12)	3.07(−12)
41, 39	2.30(−17)	4.35(−17)	4.87(−17)	1.36(−16)	5.14(−15)	1.67(−13)	9.87(−13)	2.71(−12)
43, 31	1.48(−18)	1.40(−17)	6.88(−17)	5.38(−16)	9.11(−15)	1.08(−13)	3.55(−13)	7.47(−13)
43, 33	8.07(−18)	7.16(−17)	3.30(−16)	2.31(−15)	3.22(−14)	3.36(−13)	1.09(−12)	2.31(−12)
43, 35	4.51(−17)	3.45(−16)	1.40(−15)	7.92(−15)	7.79(−14)	6.37(−13)	1.86(−12)	3.68(−12)
43, 37	3.67(−16)	1.86(−15)	5.39(−15)	1.88(−14)	9.16(−14)	6.44(−13)	2.04(−12)	4.24(−12)
43, 39	1.93(−16)	2.81(−16)	3.58(−16)	1.24(−15)	1.85(−14)	3.09(−13)	1.45(−12)	3.62(−12)
43, 41	1.53(−12)	4.03(−12)	7.37(−12)	1.57(−11)	4.00(−11)	8.15(−11)	1.10(−10)	1.31(−10)
45, 31	9.55(−19)	6.74(−18)	2.19(−17)	1.67(−16)	4.62(−15)	7.89(−14)	2.92(−13)	6.32(−13)
45, 33	3.46(−18)	2.70(−17)	1.02(−16)	8.09(−16)	1.82(−14)	2.53(−13)	8.60(−13)	1.80(−12)
45, 35	1.58(−17)	1.28(−16)	5.27(−16)	3.85(−15)	6.32(−14)	6.73(−13)	2.11(−12)	4.26(−12)
45, 37	2.09(−16)	1.41(−15)	4.78(−15)	2.47(−14)	2.46(−13)	1.76(−12)	4.61(−12)	8.44(−12)
45, 39	1.54(−14)	4.50(−14)	8.86(−14)	2.02(−13)	5.39(−13)	1.64(−12)	4.03(−12)	7.63(−12)
45, 41	1.59(−14)	6.81(−14)	1.78(−13)	6.29(−13)	3.20(−12)	1.18(−11)	2.06(−11)	2.80(−11)
45, 43	2.78(−13)	9.75(−13)	2.18(−12)	6.01(−12)	2.14(−11)	5.84(−11)	9.08(−11)	1.17(−10)
47, 31	5.00(−19)	3.63(−18)	1.02(−17)	4.71(−17)	1.49(−15)	4.04(−14)	1.84(−13)	4.37(−13)
47, 33	3.29(−19)	3.93(−18)	2.02(−17)	1.93(−16)	6.56(−15)	1.42(−13)	5.74(−13)	1.29(−12)
47, 35	2.61(−18)	2.86(−17)	1.35(−16)	1.07(−15)	2.61(−14)	4.17(−13)	1.45(−12)	2.98(−12)
47, 37	3.43(−17)	3.25(−16)	1.34(−15)	8.15(−15)	1.23(−13)	1.36(−12)	4.06(−12)	7.72(−12)
47, 39	1.44(−15)	1.03(−14)	3.35(−14)	1.31(−13)	8.90(−13)	5.48(−12)	1.28(−11)	2.12(−11)
47, 311.....	7.76(−14)	2.02(−13)	3.36(−13)	5.96(−13)	1.13(−12)	2.44(−12)	5.38(−12)	9.96(−12)
47, 41	1.19(−16)	7.62(−16)	3.45(−15)	2.38(−14)	2.59(−13)	1.77(−12)	4.07(−12)	6.42(−12)
47, 43	2.24(−15)	1.23(−14)	3.94(−14)	1.86(−13)	1.42(−12)	7.35(−12)	1.50(−11)	2.23(−11)
47, 45	6.18(−14)	2.70(−13)	6.86(−13)	2.25(−12)	1.04(−11)	3.64(−11)	6.29(−11)	8.55(−11)

TABLE 8

SAME AS TABLE 2, BUT FOR THE $v = 5$ LEVEL OF PARA-H_2

	T (K)							
vj, $v'j'$	100	200	300	500	1000	2000	3000	4000
50, 40	1.23(−17)	8.75(−17)	3.31(−16)	1.89(−15)	1.99(−14)	1.96(−13)	6.65(−13)	1.42(−12)
50, 42	3.17(−17)	1.93(−16)	6.23(−16)	2.74(−15)	2.29(−14)	2.42(−13)	8.78(−13)	1.98(−12)
50, 44	1.64(−17)	1.12(−16)	4.80(−16)	3.73(−15)	5.15(−14)	4.44(−13)	1.34(−12)	2.77(−12)
50, 46	3.24(−17)	2.40(−16)	9.18(−16)	5.33(−15)	6.73(−14)	7.11(−13)	2.18(−12)	4.29(−12)
50, 48	6.41(−18)	3.94(−17)	1.27(−16)	1.15(−15)	3.02(−14)	5.90(−13)	2.31(−12)	4.98(−12)
52, 40	2.26(−18)	1.83(−17)	8.29(−17)	6.33(−16)	8.65(−15)	7.84(−14)	2.39(−13)	4.87(−13)
52, 42	1.64(−17)	1.26(−16)	5.42(−16)	3.80(−15)	4.74(−14)	4.42(−13)	1.41(−12)	2.94(−12)
52, 44	6.94(−17)	4.57(−16)	1.71(−15)	9.79(−15)	9.28(−14)	6.81(−13)	1.94(−12)	3.81(−12)
52, 46	2.19(−16)	1.08(−15)	3.09(−15)	1.28(−14)	1.08(−13)	9.34(−13)	2.73(−12)	5.24(−12)
52, 48	1.17(−15)	1.87(−15)	2.35(−15)	5.07(−15)	5.30(−14)	7.47(−13)	2.73(−12)	5.74(−12)
52, 50	3.56(−12)	7.67(−12)	1.22(−11)	2.14(−11)	4.10(−11)	6.52(−11)	7.91(−11)	8.83(−11)
54, 40	7.79(−19)	6.74(−18)	3.33(−17)	3.07(−16)	5.92(−15)	6.67(−14)	2.02(−13)	3.92(−13)
54, 42	6.78(−18)	5.55(−17)	2.59(−16)	2.21(−15)	3.66(−14)	3.71(−13)	1.10(−12)	2.13(−12)
54, 44	3.45(−17)	2.58(−16)	1.10(−15)	8.04(−15)	1.06(−13)	9.36(−13)	2.71(−12)	5.25(−12)
54, 46	2.34(−16)	1.50(−15)	5.47(−15)	3.04(−14)	2.76(−13)	1.84(−12)	4.74(−12)	8.54(−12)
54, 48	6.95(−15)	2.46(−14)	5.43(−14)	1.43(−13)	4.78(−13)	1.99(−12)	5.05(−12)	9.23(−12)
54, 50	5.00(−14)	1.76(−13)	4.04(−13)	1.16(−12)	4.17(−12)	1.08(−11)	1.59(−11)	1.95(−11)
54, 52	9.19(−13)	2.73(−12)	5.56(−12)	1.34(−11)	3.82(−11)	8.44(−11)	1.18(−10)	1.42(−10)
56, 40	1.54(−19)	1.45(−18)	7.81(−18)	9.33(−17)	2.81(−15)	4.66(−14)	1.60(−13)	3.21(−13)
56, 42	1.38(−18)	1.25(−17)	6.44(−17)	7.14(−16)	1.89(−14)	2.73(−13)	8.89(−13)	1.74(−12)
56, 44	7.87(−18)	6.56(−17)	3.10(−16)	2.95(−15)	6.15(−14)	7.07(−13)	2.10(−12)	3.95(−12)
56, 46	6.19(−17)	4.54(−16)	1.88(−15)	1.41(−14)	2.11(−13)	1.86(−12)	5.06(−12)	9.16(−12)
56, 48	1.10(−15)	6.32(−15)	2.06(−14)	1.03(−13)	9.03(−13)	5.29(−12)	1.21(−11)	2.00(−11)
56, 410.....	1.52(−13)	3.13(−13)	5.00(−13)	8.93(−13)	1.74(−12)	3.69(−12)	7.34(−12)	1.24(−11)
56, 50	8.52(−16)	4.58(−15)	1.48(−14)	6.69(−14)	4.50(−13)	2.01(−12)	3.72(−12)	5.15(−12)
56, 52	1.09(−14)	5.33(−14)	1.59(−13)	6.33(−13)	3.50(−12)	1.34(−11)	2.35(−11)	3.18(−11)
56, 54	1.83(−13)	6.98(−13)	1.72(−12)	5.24(−12)	2.00(−11)	5.64(−11)	8.79(−11)	1.13(−10)

TABLE 9

SAME AS TABLE 8, BUT FOR ORTHO-H_2

	T (K)							
vj, $v'j'$	100	200	300	500	1000	2000	3000	4000
51, 41	6.91(−18)	5.48(−17)	2.48(−16)	1.86(−15)	2.71(−14)	3.17(−13)	1.15(−12)	2.60(−12)
51, 43	3.01(−17)	2.04(−16)	7.83(−16)	4.50(−15)	4.39(−14)	3.84(−13)	1.29(−12)	2.83(−12)
51, 45	3.41(−17)	1.79(−16)	6.06(−16)	3.63(−15)	5.32(−14)	5.98(−13)	1.90(−12)	3.85(−12)
51, 47	7.16(−17)	2.16(−16)	6.51(−16)	3.60(−15)	4.13(−14)	5.31(−13)	1.94(−12)	4.15(−12)
53, 41	2.75(−18)	2.17(−17)	1.02(−16)	8.29(−16)	1.39(−14)	1.69(−13)	5.85(−13)	1.27(−12)
53, 43	1.52(−17)	1.14(−16)	5.01(−16)	3.72(−15)	5.33(−14)	5.62(−13)	1.87(−12)	3.98(−12)
53, 45	8.49(−17)	5.52(−16)	2.14(−15)	1.29(−14)	1.33(−13)	1.04(−12)	2.94(−12)	5.65(−12)
53, 47	8.40(−16)	3.52(−15)	9.33(−15)	3.12(−14)	1.50(−13)	9.87(−13)	2.98(−12)	5.91(−12)
53, 49	1.15(−17)	1.32(−16)	4.77(−16)	2.99(−15)	3.34(−14)	4.09(−13)	1.69(−12)	3.95(−12)
53, 51	1.80(−12)	4.22(−12)	8.04(−12)	1.87(−11)	4.81(−11)	9.27(−11)	1.21(−10)	1.41(−10)
55, 41	5.66(−19)	5.21(−18)	2.77(−17)	2.75(−16)	6.23(−15)	9.66(−14)	3.66(−13)	8.15(−13)
55, 43	3.12(−13)	9.90(−13)	2.46(−12)	7.70(−12)	2.76(−11)	7.04(−11)	1.05(−10)	1.31(−10)
55, 45	2.42(−17)	1.86(−16)	8.49(−16)	6.49(−15)	9.69(−14)	1.00(−12)	3.11(−12)	6.20(−12)
55, 47	3.32(−16)	2.03(−15)	7.60(−15)	4.29(−14)	4.04(−13)	2.75(−12)	6.95(−12)	1.23(−11)
55, 49	3.26(−14)	8.47(−14)	1.63(−13)	3.69(−13)	8.94(−13)	2.21(−12)	4.81(−12)	8.61(−12)
55, 51	2.17(−14)	8.85(−14)	2.60(−13)	1.00(−12)	4.85(−12)	1.58(−11)	2.57(−11)	3.34(−11)
55, 53	3.12(−13)	9.90(−13)	2.46(−12)	7.70(−12)	2.76(−11)	7.04(−11)	1.05(−10)	1.31(−10)
57, 41	6.70(−20)	8.04(−19)	5.19(−18)	6.21(−17)	1.95(−15)	4.12(−14)	1.81(−13)	4.40(−13)
57, 43	4.14(−19)	4.62(−18)	2.80(−17)	3.12(−16)	8.54(−15)	1.55(−13)	6.06(−13)	1.36(−12)
57, 45	3.13(−18)	3.11(−17)	1.73(−16)	1.63(−15)	3.44(−14)	4.79(−13)	1.64(−12)	3.38(−12)
57, 47	4.32(−17)	3.48(−16)	1.63(−15)	1.21(−14)	1.73(−13)	1.68(−12)	4.93(−12)	9.35(−12)
57, 49	2.18(−15)	1.20(−14)	4.13(−14)	2.00(−13)	1.48(−12)	7.91(−12)	1.74(−11)	2.77(−11)
57, 411.....	4.40(−14)	1.37(−13)	3.02(−13)	7.59(−13)	1.78(−12)	3.70(−12)	7.19(−12)	1.22(−11)
57, 51	3.06(−16)	2.16(−15)	9.32(−15)	5.57(−14)	5.07(−13)	2.91(−12)	6.05(−12)	8.98(−12)
57, 53	2.74(−15)	1.68(−14)	6.63(−14)	3.40(−13)	2.36(−12)	1.07(−11)	2.03(−11)	2.89(−11)
57, 55	5.70(−14)	2.50(−13)	8.00(−13)	3.15(−12)	1.45(−11)	4.61(−11)	7.56(−11)	9.97(−11)

TABLE 10

SAME AS TABLE 2, BUT FOR THE $v = 6$ LEVEL OF PARA-H_2

	T (K)							
vj, $v'j'$	100	200	300	500	1000	2000	3000	4000
60, 50	3.91(−17)	2.58(−16)	9.12(−16)	4.70(−15)	4.39(−14)	3.92(−13)	1.20(−12)	2.36(−12)
60, 52	9.56(−17)	5.25(−16)	1.54(−15)	6.05(−15)	4.77(−14)	4.69(−13)	1.56(−12)	3.27(−12)
60, 54	7.24(−17)	4.31(−16)	1.61(−15)	1.01(−14)	1.06(−13)	7.79(−13)	2.21(−12)	4.29(−12)
60, 56	8.01(−17)	6.49(−16)	2.51(−15)	1.41(−14)	1.52(−13)	1.28(−12)	3.51(−12)	6.43(−12)
60, 58	1.06(−17)	9.97(−17)	3.72(−16)	3.62(−15)	8.20(−14)	1.22(−12)	4.05(−12)	7.86(−12)
62, 50	8.18(−18)	6.30(−17)	2.69(−16)	1.81(−15)	1.99(−14)	1.51(−13)	4.21(−13)	7.95(−13)
62, 52	5.18(−17)	3.84(−16)	1.57(−15)	9.81(−15)	1.03(−13)	8.42(−13)	2.46(−12)	4.76(−12)
62, 54	1.92(−16)	1.24(−15)	4.41(−15)	2.28(−14)	1.84(−13)	1.18(−12)	3.13(−12)	5.81(−12)
62, 56	6.88(−16)	3.38(−15)	9.41(−15)	3.55(−14)	2.49(−13)	1.71(−12)	4.43(−12)	7.89(−12)
62, 58	2.78(−15)	4.22(−15)	5.52(−15)	1.35(−14)	1.34(−13)	1.52(−12)	4.76(−12)	9.07(−12)
62, 60	4.62(−12)	9.70(−12)	1.52(−11)	2.58(−11)	4.67(−11)	7.02(−11)	8.32(−11)	9.15(−11)
64, 50	3.16(−18)	2.58(−17)	1.21(−16)	1.01(−15)	1.54(−14)	1.33(−13)	3.52(−13)	6.23(−13)
64, 52	2.48(−17)	1.92(−16)	8.51(−16)	6.55(−15)	8.78(−14)	7.09(−13)	1.87(−12)	3.34(−12)
64, 54	1.11(−16)	7.90(−16)	3.20(−15)	2.10(−14)	2.32(−13)	1.71(−12)	4.50(−12)	8.12(−12)
64, 56	6.66(−16)	4.00(−15)	1.38(−14)	6.94(−14)	5.40(−13)	3.13(−12)	7.42(−12)	1.26(−11)
64, 58	1.75(−14)	5.94(−14)	1.27(−13)	3.15(−13)	9.72(−13)	3.67(−12)	8.42(−12)	1.42(−11)
64, 60	8.78(−14)	3.00(−13)	6.61(−13)	1.77(−12)	5.70(−12)	1.31(−11)	1.82(−11)	2.15(−11)
64, 62	1.39(−12)	4.08(−12)	7.96(−12)	1.81(−11)	4.76(−11)	9.73(−11)	1.31(−10)	1.53(−10)
66, 50	7.42(−19)	7.00(−18)	3.71(−17)	3.85(−16)	8.71(−15)	1.04(−13)	2.96(−13)	5.26(−13)
66, 52	6.07(−18)	5.50(−17)	2.80(−16)	2.69(−15)	5.38(−14)	5.76(−13)	1.59(−12)	2.80(−12)
66, 54	2.98(−17)	2.50(−16)	1.17(−15)	9.73(−15)	1.55(−13)	1.37(−12)	3.56(−12)	6.12(−12)
66, 56	1.97(−16)	1.44(−15)	5.94(−15)	3.99(−14)	4.68(−13)	3.36(−12)	8.21(−12)	1.38(−11)
66, 58	2.82(−15)	1.60(−14)	5.18(−14)	2.42(−13)	1.73(−12)	8.66(−12)	1.83(−11)	2.86(−11)
66, 510.....	2.94(−13)	6.00(−13)	9.23(−13)	1.55(−12)	2.85(−12)	6.08(−12)	1.16(−11)	1.83(−11)
66, 60	1.98(−15)	1.01(−14)	3.02(−14)	1.25(−13)	7.44(−13)	2.79(−12)	4.66(−12)	6.08(−12)
66, 62	2.23(−14)	1.05(−13)	2.86(−13)	1.03(−12)	5.25(−12)	1.77(−11)	2.86(−11)	3.68(−11)
66, 64	3.06(−13)	1.15(−12)	2.60(−12)	7.11(−12)	2.56(−11)	6.81(−11)	1.01(−10)	1.25(−10)

TABLE 11

SAME AS TABLE 10, BUT FOR ORTHO-H_2

	T (K)							
vj, $v'j'$	100	200	300	500	1000	2000	3000	4000
61, 51	2.13(−17)	1.66(−16)	7.25(−16)	5.02(−15)	6.40(−14)	6.64(−13)	2.21(−12)	4.57(−12)
61, 53	8.24(−17)	5.33(−16)	1.95(−15)	1.03(−14)	8.87(−14)	7.30(−13)	2.32(−12)	4.79(−12)
61, 55	1.22(−16)	5.99(−16)	1.92(−15)	1.03(−14)	1.23(−13)	1.13(−12)	3.25(−12)	6.16(−12)
61, 57	2.61(−16)	6.80(−16)	1.86(−15)	9.35(−15)	9.55(−14)	1.04(−12)	3.39(−12)	6.68(−12)
63, 51	9.64(−18)	7.36(−17)	3.26(−16)	2.43(−15)	3.49(−14)	3.55(−13)	1.11(−12)	2.21(−12)
63, 53	4.74(−17)	3.42(−16)	1.43(−15)	9.69(−15)	1.20(−13)	1.10(−12)	3.38(−12)	6.71(−12)
63, 55	2.32(−16)	1.47(−15)	5.38(−15)	2.95(−14)	2.68(−13)	1.84(−12)	4.84(−12)	8.84(−12)
63, 57	2.51(−15)	1.03(−14)	2.55(−14)	7.71(−14)	3.31(−13)	1.88(−12)	5.10(−12)	9.35(−12)
63, 59	9.22(−18)	1.47(−16)	8.79(−16)	7.31(−15)	7.79(−14)	8.44(−13)	3.06(−12)	6.47(−12)
63, 61	2.54(−12)	6.12(−12)	1.14(−11)	2.46(−11)	5.79(−11)	1.04(−10)	1.31(−10)	1.49(−10)
65, 51	2.30(−18)	2.07(−17)	1.02(−16)	9.05(−16)	1.72(−14)	2.19(−13)	7.27(−13)	1.47(−12)
65, 53	1.21(−17)	1.01(−16)	4.83(−16)	3.95(−15)	6.42(−14)	6.82(−13)	2.08(−12)	4.04(−12)
65, 55	7.34(−17)	5.52(−16)	2.38(−15)	1.67(−14)	2.15(−13)	1.89(−12)	5.34(−12)	9.96(−12)
65, 57	8.69(−16)	5.24(−15)	1.84(−14)	9.48(−14)	7.83(−13)	4.66(−12)	1.09(−11)	1.82(−11)
65, 59	7.70(−14)	1.97(−13)	3.61(−13)	7.44(−13)	1.63(−12)	3.86(−12)	7.95(−12)	1.33(−11)
65, 61	4.24(−14)	1.81(−13)	4.90(−13)	1.68(−12)	7.10(−12)	2.03(−11)	3.07(−11)	3.82(−11)
65, 63	4.98(−13)	1.68(−12)	3.91(−12)	1.10(−11)	3.54(−11)	8.29(−11)	1.18(−10)	1.43(−10)
67, 51	3.29(−19)	3.73(−18)	2.16(−17)	2.33(−16)	6.03(−15)	1.02(−13)	3.87(−13)	8.41(−13)
67, 53	1.58(−18)	1.63(−17)	1.04(−16)	1.08(−15)	2.44(−14)	3.50(−13)	1.18(−12)	2.41(−12)
67, 55	1.15(−17)	1.08(−16)	5.59(−16)	4.82(−15)	8.56(−14)	9.75(−13)	2.93(−12)	5.57(−12)
67, 57	1.40(−16)	1.09(−15)	4.62(−15)	3.08(−14)	3.74(−13)	3.08(−12)	8.17(−12)	1.45(−11)
67, 59	5.74(−15)	3.10(−14)	9.76(−14)	4.25(−13)	2.75(−12)	1.28(−11)	2.59(−11)	3.92(−11)
67, 511.....	4.76(−14)	2.19(−13)	4.93(−13)	1.17(−12)	2.68(−12)	5.86(−12)	1.12(−11)	1.81(−11)
67, 61	8.54(−16)	6.05(−15)	2.27(−14)	1.19(−13)	9.11(−13)	4.19(−12)	7.78(−12)	1.08(−11)
67, 63	6.50(−15)	4.07(−14)	1.38(−13)	6.19(−13)	3.73(−12)	1.44(−11)	2.51(−11)	3.39(−11)
67, 65	1.06(−13)	4.94(−13)	1.39(−12)	4.74(−12)	1.96(−11)	5.63(−11)	8.72(−11)	1.11(−10)

coefficients for ro-vibrational transitions involving $\Delta j = -4\Delta v$ predominate over other transitions where changes in both v and j occur. This is clearly seen for (vj, $v'j'$) transitions with $\Delta v = v' - v = -1$ for $j = 3$–7, and the effect becomes stronger with increasing rotational excitation but less important as T increases. This is an example of quasi-resonant scattering (Stewart et al. 1988; Forrey et al. 1999). A detailed study of this process in the limit of zero temperature and its correspondence with classical mechanics has been carried out recently (Forrey et al. 1999). The efficient conversion of vibrational energy into rotational energy may produce a significant population of high rotational levels in environments where molecular hydrogen is subjected to an intense flux of X-rays or ultraviolet photons.

This work was supported by the National Science Foundation (NSF), Division of Astronomy. M. V. was supported by the NSF through the Research Experience for Undergraduates program at the Smithsonian Astrophysical Observatory.

REFERENCES

Alexander, M. H. 1976, Chem. Phys. Lett., 38, 417
———. 1977, J. Chem. Phys., 66, 4608
Alexander, M. H., & McGuire, P. 1976, J. Chem. Phys., 64, 452
Audibert, M. M., Vilaseca, R., Lukasik, J., & Ducuing, J. 1976, Chem. Phys. Lett., 37, 408
Balakrishnan, N., Forrey, R. C., & Dalgarno, A. 1998, Phys. Rev. Lett., 80, 3224
———. 1999, ApJ, 514, 520
Blais, N. C., & Truhlar, D. G. 1976, J. Chem. Phys., 65, 5335
Bujarrabal, V., Alcolea, J., Sahai, R., Zamorano, J., & Zijlstra, A. A. 1998, A&A, 331, 361
Dalgarno, A. 1995, in ASP Conf. Ser. 80, The Physics of the Interstellar Medium and Intergalactic Medium, ed. A. Ferrara, C. Heiles, C. McKee, & P. Shapiro (San Francisco: ASP), 37
Dove, J. E., Raynor, S., & Teitelbaum, H. 1980, Chem. Phys., 50, 175
Dubernet, M.-L., & Tuckey, P. A. 1999, Chem. Phys. Lett., 300, 275
Eastes, W., & Secrest, D. 1972, J. Chem. Phys., 56, 640
Flower, D. R., Roueff, E., & Zeippen, C. J. 1998, J. Phys. B, 31, 1105
Forrey, R. C., Balakrishnan, N., Dalgarno, A., Haggerty, M. R., & Heller, E. J. 1999, Phys. Rev. Lett., 82, 2657
Hutson, J. M., & Green, S. 1994, MOLSCAT ver. 14 (distributed by Collaborative Computational Project 6; Daresbury Laboratory: UK Eng. Phys. Sci. Res. Council)
Krauss, M., & Mies, F. H. 1965, J. Chem. Phys., 42, 2703
Lepp, S., Buch, V., & Dalgarno, A. 1995, ApJS, 98, 345
McGuire, P., & Kouri, D. J. 1974, J. Chem. Phys., 60, 2488
Michaut, X., Saint-Loup, R., Berger, H., Dubernet, M. L., Joubert, P., & Bonamy, J. 1998, J. Chem. Phys., 109, 951
Muchnick, P., & Russek, A. 1994, J. Chem. Phys., 100, 4336
Raczkowski, A. W., Lester, W. A., Jr., & Miller, W. H. 1978, J. Chem. Phys., 69, 2692
Schwenke, D. W. 1988, J. Chem. Phys., 89, 2076
Shupe, D. L., Larkin, J. E., Knop, R. A., Armus, L., Matthews, K., & Soifer, B. T. 1998, ApJ, 498, 267
Stanke, T., McCaughrean, M. J., & Zinnecker, H. 1998, A&A, 332, 307
Stewart, B., Magill, P. D., Scott, T. P., Derouard, J., & Pritchard, D. E. 1988, Phys. Rev. Lett., 60, 282
van Dishoeck, E. F., et al. 1998, ApJ, 502, L173
Weintraub, D. A., Huard, T., Kastner, J. H., & Gatley, I. 1998, ApJ, 509, 728